

# SYNTHESIS OF PFG BRAND CORROSION INHIBITOR AND ITS QUANTUM CHEMICAL CALCULATION RESULTS

A.K. Nomozov<sup>1\*</sup>, Kh.S. Beknazarov<sup>2</sup>, Y.A. Geldiev<sup>3</sup>, B.E. Babamurodov<sup>4</sup>, N.Sh. Muzaffarova<sup>5</sup>, S.G. Yuldashova<sup>5</sup>

<sup>1</sup>Department of Chemical Technology, Termez State University of Engineering and Agrotechnologies, Termez, 190111 Uzbekistan

<sup>2</sup>Angreen University, Tashkent, Uzbekistan

<sup>3</sup>Faculty of Chemistry, Termez State University, Uzbekistan, Termez, 190111 Uzbekistan
<sup>4</sup>Faculty of Medical, Termez University of Economics and Service, Termez, 190111 Uzbekistan
<sup>5</sup>Department of Medical and Biological Chemistry, Termez branch of Tashkent Medical Academy, Termez, 190111 Uzbekistan

\*e-mail: abrornomozov055@gmail.com

Received 22.07.2024 Accepted 13.09.2024

Abstract: This article examines the optimal conditions for synthesizing a new type of corrosion inhibitor based on p-paraphenylenediamine, formalin, and glycine. It was determined that the ideal mole ratio of the initial substances is 1:2:2 mol, and the optimal temperature range is between 40 and 65 degrees Celsius. The reaction efficiency under these optimal conditions was found to be 89.4%. The structure of the synthesized corrosion inhibitor was analyzed using IR spectra. Additionally, the Avogadro, Hyper Chem 8.01, Asselrys MS Modeling 3.0.1 software was used to perform quantum chemical calculations on the reaction properties of this synthesized inhibitor molecule. The calculations were carried out using the constrained Semi-empirical (UHF) method, with SCF-MO using semi-empirical AM1, MNDO, and PM3. These calculations were performed on an Intel Pro Pentium 1.40 GHz computer, utilizing the RM1, MNDO3 HOMO, and LUMO methods. To further evaluate the effectiveness of this synthesized corrosion inhibitor, the gravimetric method was employed to inhibit St20 grade steel in a 1 M HCl solution. The steel surface morphology and element composition were also examined using SEM and AFM analysis.

Keywords: p-paraphenylenediamine, formalin, glycine, corrosion inhibitor, SEM and AFM analysis.

DOI: 10.32737/2221-8688-2025-3-297-309

#### Introduction

Corrosion inhibitors are widely used to protect metals against various corrosive environments [1, 2]. A corrosion inhibitor is a compound that is added in low concentrations to a corrosive solution to reduce and/or minimize the corrosion rate [3]. Amines are the main part of organic substances that are among the inhibitors that reduce the process of corrosion of metals under the influence of the external environment. The inhibitory properties various amines have been widely studied [4, 5]. Complexes of 4-[(2,4-dihydroxy-benzylidene)amino]-1, 5-dimethyl-2-phenyl-1, 2-dihydroxypyrazole-3- with various metals exhibit mixed inhibitory properties in 2 M HCl acid medium shows. It showed inhibition efficiency of 85.1% at a concentration of 11·10-6 mol/l [6]. The

inhibition properties of N,N-dipropinoxy methyl amine trimethylphosphonate were studied using potentiometric polarization curves electrochemical methods. In this study, at a temperature of 298 K, concentrations ranging from 40 mg/l to 320 mg/l, this inhibitor was classified as a mixed type inhibitor [7]. Also, a number of ammonium compounds, namely N [isononylphenoxypoly (ethyleneoxy) carbonylmethyl] chloride, ammonium cationic surfactants: 1-methyl-3-tetradecyl imidazolium bromide, 1-methyl-3-hexadexyl imidazolium bromide, N,N-tetradecyl pyridinium. bromide, N,N-hexadecyl pyridinium bromide, N,N-dimethyl ammoyldimethyl bromide, N,N-dimethyl-N-ethylbenzyl ammonium laurate N,N-dimethyl-Nand

ethylbenzyl ammonium acetate compounds from various compounds (10, 25, 50, 100 and 200 mg) concentrations of API 5L X52 grade steel in 2 M hydrochloric acid inhibition efficiency of more than 90%, imidazoline-based dissymmetric and bis-symmetric ammonium salt (DBA) and thiourea modification Nhydroxy ethylated ammonium salts have been used to prevent hydrogen-sulfide corrosion, showing an efficiency of Z = 95 to 97 % [8, 9]. Pyrazol[3,4-d]pyrimidnone compound was used as an effective corrosion inhibitor for corrosion protection of carbon steel in 1.0 M HCl solution [10]. From the following diblock copolymers based on ethyl methacrylate and amines: poly[2(dimethylamino)ethyl methacrylate] poly[2-(diethylamino) (PDMA),

methacrylate] (PDEA), poly[2-(diisopropylamino)ethyl methacrylate] (PDPA) homopolymers and polydimethylamino (poly [2-)ethylmethacrylate]-βpoly[methylmethacrylate] (PDMA-β-PMMA), poly[2-(diethylamino)ethylmethacrylate]-βpoly[methylmethacrylate] (PDEA-β-PDMA) and poly[2-( used diisopropylaminolate)-βpoly[2-(dimethylamino)ethyl methacrylate] (PDPA-β-PDMA) compounds as effective corrosion inhibitors for corrosion protection of

The purpose of this study is to synthesize a corrosion inhibitor based on P-paraphenylenediamine, formalin, and glycine the quantum chemical calculation of the reaction properties.

# **Experimental part**

Materials. Compounds of pparaphenylenediamine, formalin, and glycine were used for this study. All chemical reagents were purchased as "chemically pure" from "Merit Chemicals" company. The experiments were carried out with samples of carbon steel grade S20 and steel samples of this brand were purchased from "Uzbekistan Metallurgical Combinat" JSC.

*Methods. IR- analysis.* In the analysis of this compound, the IR-spectra produced by the Bruker company in Germany were used.

Quantum chemical analysis. Quantum-chemical calculation of the reactivity of the corrosion inhibitor molecule using Avogadro, Hyper Chem 8.01, Asselrys MS Modeling 3.0.1 using the constrained Semi-empirical (DFT) method, semi-empirical AM1, MNDO, PM3, RM1 and MINDO3 using SCF-MO calculations were carried out using the Intel Pro Pentium

1.40 GHz computer.

AISI 304 steel [11-16].

SEM and AFM analysis. Surface morphology and microstructure studies of the samples were carried out using a scanning electron microscope SEM-EVO MA 10 (Carl Zeiss, made in Germany) and Agilent 5500 (Agilent, USA) atomic force microscope (AFM).

Synthesis of inhibitor. In the synthesis of this corrosion inhibitor, 0.1 mol of amine and 0.2 mol of formalin were added slowly from a solution of 0.2 mol of glycine dissolved in double-distilled water with stirring at 40 and 45 °C for 45 minutes in the presence of a reflux refrigerator in a nitrogen atmosphere. During this process, the temperature was in the range of 55-65 °C. The yield of this reaction mainly depends on the mole ratio of the starting materials and the temperature of the reaction medium (Table 1).

**Table 1.** Dependence of the synthesis yield of PFG brand corrosion inhibitor on the mole ratio of starting materials and temperature.

p-phenylenediamine	Temperature <sup>0</sup> C	Yield %	Temperature <sup>0</sup> C	Yield %
formalin+glycine				
1:1:1		49.67		23.35
1:2:2		89,4		61.36
2:2:1	40÷65	56.15	65≤t	32.26
2:1:3		32.62		29.56
1:2:1		39.43		33.25

As can be seen from Table 1, the highest productivity was achieved when the temperature was in the range of 40÷65 °C and the mole ratio of the starting materials was 1:2:2. As the temperature increased to 65 °C, the product yield also decreased significantly. In conclusion, it can be said that one of the most important factors after the temperature is the mole ratio of the initial substances. The yield of the obtained product was 89.4 percent. The resulting compound is well soluble in water, ethanol, and dimethylformamide at a temperature above 40 °C.

IR spectrum analysis of inhibitor. It has been determined that the effectiveness of the

inhibitors depends on the fact that they are adsorbed on the surface of steel and form chemical compounds with iron ions that are poorly soluble due to the functional groups in the composition. In addition, the structure of the molecule, the length of the oligomer chain is also important. Therefore, in order to discuss the mechanism of inhibition, we need to know the structure of the molecules of the obtained inhibitors. The structure of substances was studied using the IR spectroscopy method. For this purpose, IR spectra of the first reactant (1,4phenylenebis(azanedyl)) dimethanol obtained, newly formed bonds and groups were identified through absorption lines (Scheme 1).

**Scheme 1.** Reaction of (1,4-phenylenebis(azanedyl)) dimethanol

In Fig. 1, the IR-(BRUKER) spectrometer results of (1,4-phenylenebis(azanedyl)) dimethanol show that in the IR-(BRUKER) spectrum of X, according to the results of the IR-spectrum, v(OH) group's valence symmetric ns and 1458.81 cm<sup>-1</sup> field, deformation d vibration frequency was formed. In the 3158.36 cm<sup>-1</sup> and 1178.36 cm<sup>-1</sup> regions, valence symmetric ns and deformation δ vibrations of

the  $v(NH_2)$  group were formed. At the same time, the frequency of valence asymmetric  $v_{as}$ , valence symmetric  $v_s$  and deformation  $\delta$  vibrations of the v(CH) bond belonging to the benzene ring at 2981.24 cm<sup>-1</sup> and 1214.28 cm<sup>-1</sup>, 2874.35 cm<sup>-1</sup> and 1443.87 cm<sup>-1</sup> fields, the frequency of valence asymmetric  $v_{as}$ , valence symmetric  $v_s$  and deformational  $\delta$  vibrations of  $v(CH_2)$  group was formed.

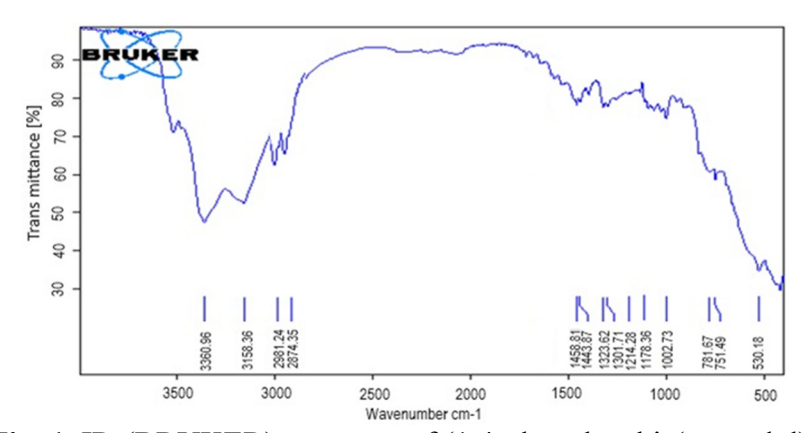


**Fig. 1.** IR-(BRUKER) spectrum of (1,4-phenylenebis(azanedyl)).

In Fig. 2, the IR-(BRUKER) spectrometer results of PFG show that in the IR-(BRUKER) spectrum of the inhibitor at 3243.67 cm<sup>-1</sup>, 3157.69 cm<sup>-1</sup>, and 1471.79 cm<sup>-1</sup>, v(NH) the

frequency of valence symmetric  $v_s$  and deformational  $\delta$  vibrations of the group was observed. Together with this, the frequency of valence asymmetric  $v_{as}$ , valence symmetric ns

and deformational  $\delta$  vibrations of the  $\nu(\text{CH}_2)$  group was formed in the areas of 2973.60 cm<sup>-1</sup>, 2892.31 cm<sup>-1</sup> and 1396.96 cm<sup>-1</sup>. In the 1608.24

cm<sup>-1</sup> area, the valence v vibration of the v(C=O) group was formed, as well as the deformation  $\delta$  vibration frequency in the 837.97 cm<sup>-1</sup> area.

Scheme 2. Synthesis of corrosion inhibitor

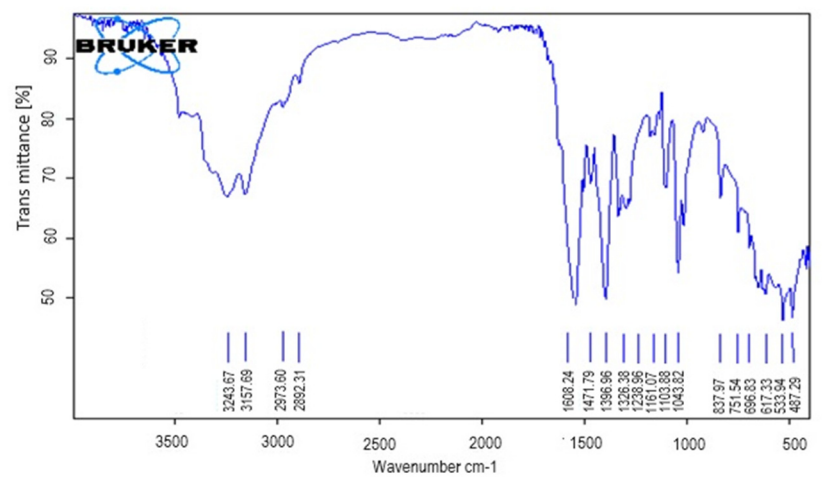


Fig. 2. IR-(BRUKER) spectrum of PFG inhibitor

Quantum chemical analysis of PFG brand corrosion inhibitor. As a result of studying the "composition-structure-property" system in chemical compounds, it is possible to theoretically estimate the properties, composition and molecular structure of complex compounds during research. Such information helps to synthesize complex compounds with selected properties, composition and structure. Quantum chemical calculation of the reactivity of the inhibitor molecule by semi-empirical (UHF) method in Avogadro, Hyper Chem 8.01, Asselrys MS Modeling 3.0.1, semi-empirical

AM1, MNDO, PM3, RM1 and MNDO3 methods using SCF-MO Calculations were performed on an Intel Pro Pentium 1.40 GHz computer. Molecular geometry optimization was carried out using the Polak-Ribiere (Conjugate gradient) algorithm. These methods make it possible to determine the total energy of the molecule and electron densities of molecular orbitals, as well as geometric optimization of the studied molecule. One of the important electronic characteristics is the Mulliken effective charges on atoms (CHARGES) and the total energy of the system (TOTAL ENERGY)

(Table 3). AM1, MNDO, PM3, RM1 and MNDO3 based on the results of quantum-chemical calculations using semi-empirical methods, it can be concluded that the high values of the negative effective charge in the PFG molecule are in the oxygen atoms of the

C=O and C-O-C groups, and the nitrogen atoms of the primary and secondary amine N-H groups indicates that these atoms can form complexes by connecting with metal through a coordination bond [17-19].

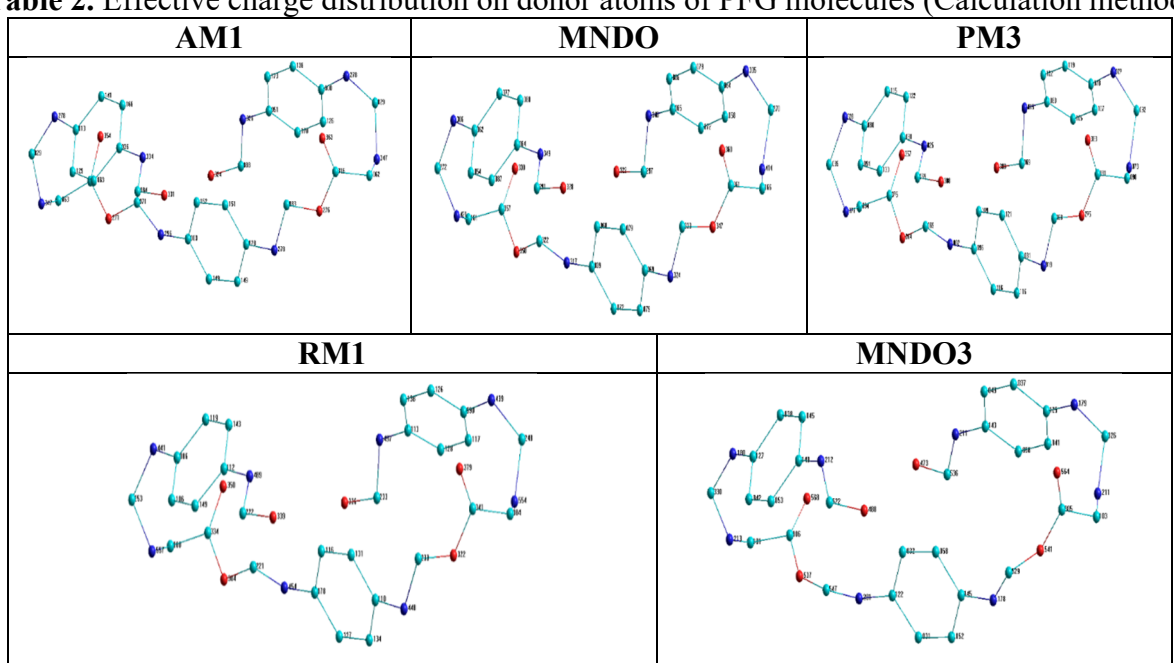


Table 2. Effective charge distribution on donor atoms of PFG molecules (Calculation method)

**Table 3.** Effective charge values of donor atoms in inhibitor molecules

Atoms	AM1, eV	MNDO, eV	PM3, eV	RM1, eV	MNDO3, eV		
PFG							
$\delta_{\mathfrak{q}}O^1\text{(C-O)}$	-0,324	-0,322	-0,308	-0,336	-0,473		
$\delta_q N^1_{(NH)}$	-0,326	-0,340	-0,015	-0,497	-0,211		
$\delta_{\mathbf{q}} N^2_{(NH)}$	-0,278	-0,305	-0,027	-0,439	-0,179		
$\delta_{\mathbf{q}} \mathbf{N}^{3}_{(\mathrm{NH})}$	-0,347	-0,414	-0,073	-0,554	-0,211		
$\delta_{\mathbf{q}}^{\mathbf{O}_{1}(C=O)}$	-0,363	-0,360	-0,383	-0,379	-0,564		
$\delta_q O^1$ (C-O C)	-0,276	-0,347	-0,275	-0,322	-0,541		
$\delta_q N^4_{(NH)}$	-0,278	-0,324	-0,019	-0,448	-0,178		
$\delta_{\mathbf{q}} \mathbf{N}^{5}_{(\mathrm{NH})}$	-0,296	-0,317	-0,002	-0,454	-0,201		
$\delta_{\mathbf{q}}^{\mathbf{O}^{2}(\text{C-O-C})}$	-0,271	-0,350	-0,264	-0,304	-0,537		
$\delta_{\mathbf{q}} \mathbf{O}^2$ (C=O)	-0,354	-0,330	-0,357	-0,350	-0,568		
$\delta_{\mathbf{q}} \mathbf{N}^{6}_{(\mathrm{NH})}$	-0,347	-0,421	-0,077	-0,557	-0,213		
$\delta_{\mathbf{q}} \mathbf{N}^{7}_{(NH)}$	-0,278	-0,306	-0,028	-0,441	-0,180		
$\delta_{\mathbf{q}} \mathbf{N}^{7}_{(NH)}$	-0,334	-0,349	-0,025	-0,489	-0,212		
$\delta_{\mathbf{q}}^{\mathbf{Q}^{2}(\text{C-O})}$	-0,331	-0,328	-0,308	-0,339	-0,488		

	-	-	-	-	-
$\mathbf{E}$	8160,2615	8153,4749	8182,9089	6884,3614	8204,4584
	(kcal/mol)	(kcal/mol)	(kcal/mol)	(kcal/mol)	(kcal/mol)

Geometric optimization of the PFG was fully optimized using the Popl basis set -RHF/6-311G(d, p) using GaussView 6.0.16 software using the out file generated by the software package. Results Avogadro GaussView 6.0.16 calculations using the DFT (B3LYP) method The Mulliken method and the frontier molecular orbital (ChegMO) approximation were used to calculate charges on all atoms. In reactivity, distribution of charge on the atoms of the molecule is important, that is, they play an important role in predicting the electrophilic and nucleophilic centers of the molecule. Taking this into account, the total charges of atoms of PFG molecules were calculated according to the widely used method of charge calculation -

Mulliken's method. The calculation results show the localization of the largest negative charge on the nitrogen and oxygen atoms of the PFG molecule (Fig. 3b).

One of the main indices used to evaluate the reactivity of organic compounds is the electron density in marginal MOs (ChegMO). The upper occupied molecular orbital (UMBO) and the lower unoccupied molecular orbital (LUMO) are frontier molecular orbitals. An atom with a high electron density in UBMO is an electron-donating atom and is an electrophilic reaction center. In LUMO, an atom with a high electron density is an electron acceptor atom and a nucleophilic reaction center.

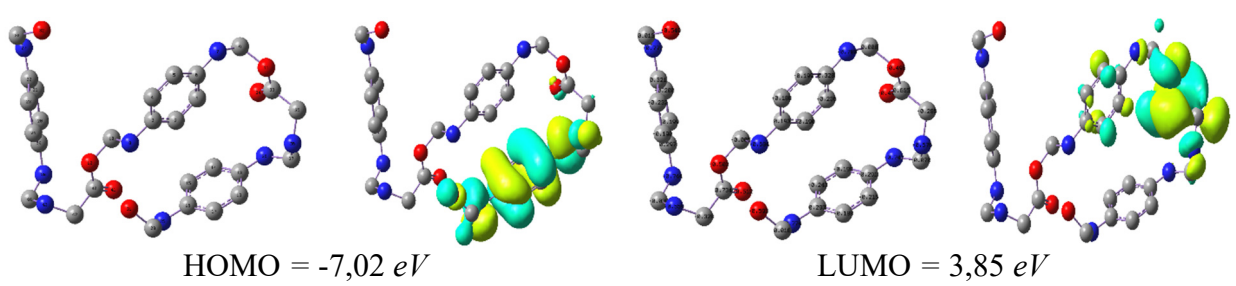


Fig. 4. Effective charge distribution on donor atoms in PFG molecules

According to the charge density of the upper occupied molecular orbital (HOMO) and the lower empty molecular orbital (LUMO), the largest distribution of charge density belongs to the -O-, C=O and N-H groups (Fig. 4 c.d).

The orbital energies of HOMO and LUMO and the difference between them ( $\Delta E=E_{LUMO}-E_{HOMO}$ , eV) are also important. An increase in the YBMO energy (increasing the occupied level towards the LUMO) in the series of compounds indicates an increase in the

electron-donating property of the compound. LUMO energy determines the electron acceptor ability (propensity for electrons) of compounds. Ionization potential, I=-E<sub>HOMO</sub>, (eV), Electron susceptibility, A=-E<sub>LUMO</sub>, (eV), Chemical hardness,  $\eta = (I-A)/2$  (eV), Chemical potential,  $\mu_p$ =-(I + A)/2 (eV), Chemical softness,  $\sigma = 1/(2\eta)$  (eV-1), Electrophilic index,  $\omega = \mu_p^2/2\eta$  (eV), Dipole moment, m (Debay) was calculated. The results are presented in Table 4.

**Table 4.** Calculated quantum chemical parameters for PFG

Quantum-chemical parameters	PFG
E <sub>номо</sub> , eV	-4.00
Elumo, eV	-0.24
$ \Delta E  = E_{LUMO} - E_{HOMO} (eV)$	3.75
Ionization potential, I=- E <sub>HOMO</sub> , (eV)	4.00
Electron susceptibility, A=-E <sub>LUMO</sub> , (eV)	0.24
Electronegativity, $\chi = (I + A)/2$ (eV)	2.12

Chemical hardness, $\eta = (I - A)/2$ (eV)	1.88
Chemical potential, $\mu_p$ =-(I + A)/2 (eV)	-2.12
Chemical softness, $\sigma = 1/(2\eta)$ (eV-1)	0.27
Electrophilic index, $\omega = \mu_p^2 / 2\eta$ (eV)	1.20
Dipole moment, μ (Debay)	4.14

It is known that the level of electrostatic potential is used to determine the electron donor and electron acceptor parts of a molecule. MEP (Molecular Electrostatic Potential) plots in red, blue, and green are negative, positive, and

neutral electrostatic potentials, respectively. Negative electrostatic potentials were formed in 110, 120, 310, 320, 410 and 25N, 26N, 28N, 36N atoms (Fig. 5).

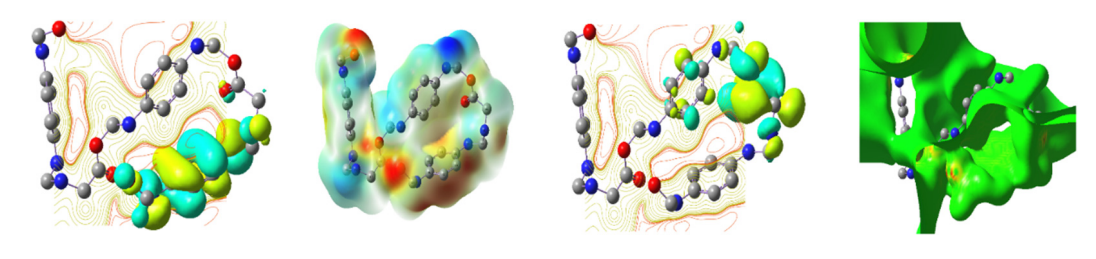


**Fig. 5.** ESP-HOMO(a), ESP-LUMO(b) and ESP(c,d) of PFG.

It is indicated that this corrosion inhibitor—splitting energy in the Fe ion orbital [20, 21]. forms low-spin complexes due to the high

#### Results and discussion

Gravimetric method. The gravimetric method is one of the widely used and effective methods for determining the corrosion rate of metal in laboratory conditions. In this case, the tested metal is determined based on the difference in mass loss in the state with and without an inhibitor added to the solution. We also conducted practical experiments at different temperatures and concentrations to determine the corrosion rate of steel. We determined the

rate of corrosion of the steel sample taken for the experiment in time intervals from 24 to 240 hours. For this purpose, experiments were carried out to determine the corrosion rate of the steel electrode at different concentrations and at certain temperatures, and the corrosion rate (K) and weight loss (X) related to the experiment in solutions with and without inhibitors were measured gravimetrically. We determined based on the method [22, 23].

$$K = \frac{(m_1 - m_2) \cdot 1000}{S \cdot \tau_1} [g/m^{-2} \cdot day]$$
 (1)

$$X = \frac{K_{\text{uhf}}}{K_0} \cdot 100, Z=100 - X, \%$$
 (2)

Here: m<sub>1</sub> is the initial weight of the metal sample, g: m<sub>2</sub> is the weight of the metal sample after exposure, g: S is the surface area of the

sample taken for the practical experiment,  $m_2$ :  $\tau_1$  is the exposure time, hours, days.

**Table 4.** The values of inhibition coefficient ( $\gamma$ ), total surface coverage ( $\theta$ ), protection level (Z) of green inhibitor in 1 M Chloride acid medium at different temperatures for 240 hours determined by gravimetric method.

gravimente memoa:								
Inhibitor	T,	С,	<i>K</i> ,	γ	Z. (%)	θ		
	(K)	(mg/l)	gr/(cm <sup>2</sup> ·hour)	•	—, ( · · )	•		

		-	1.27	-	-	-
		200	0.264	4.81	79.15	0.7915
	293	400	0.226	5.62	82.21	0.8221
		600	0.174	7.29	86.23	0.8523
		1000	0.131	9.69	89.61	0.8961
		-	1.54	-	-	-
		200	0.311	4.95	79.79	0.7979
	313	400	0.238	5.97	83.23	0.8323
		600	0.183	8.41	88.11	0.8811
PFA		1000	0.142	10.84	90.12	0.9012
ITA	323	-	1.78	-	-	-
		200	0.353	5.04	80.16	0.8016
		400	0.249	6.62	84.85	0.8485
		600	0.193	9.22	89.15	0.9015
		1000	0.159	13.11	91.21	0.9121
		-	1.94		-	-
		200	0.372	5.21	80.89	0.8089
	333	400	0.263	7.11	85.65	0.8765
		600	0.201	9.65	91.44	0.9144
		1000	0.173	14.58	93.82	0.9382

The maximum inhibition efficiency of the PFG brand corrosion inhibitor in 1 M Chloride acidic medium was 93.82% at 1000 mg/l concentration and 333 K temperature.

**SEM** analysis. The pre-corrosion, post-corrosion and inhibited conditions of the steel

surface were studied using an SEM-EVO MA 10 (Zeiss, Germany) scanning electron microscope. The surface surface of St20 steel samples at different concentrations was studied by the morphological SEM method.



**Fig 5a.** Original photograph of the steel sample

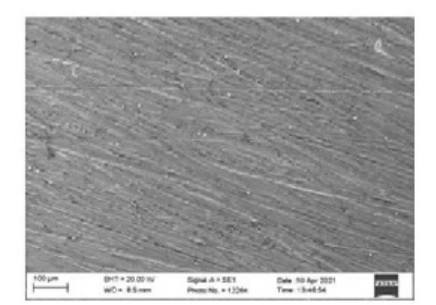


**Fig 5b.** SEM photograph of a steel sample

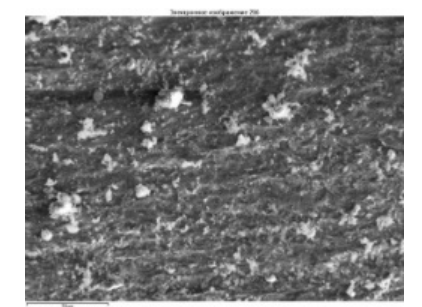


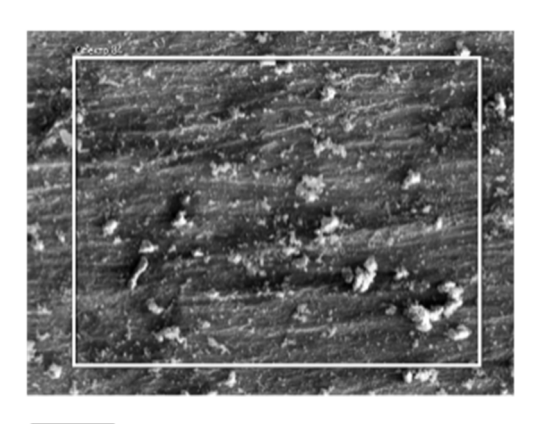
**Fig 5c.** SEM photograph of annealed steel sample

As you can see from the pictures given above, Fig. 5a shows the first photo of a steel sample cleaned with different grades of sandpaper and washed in acetone. Also, microphotographs of the original steel sample were taken using a scanning electron microscope in an environment without an inhibitor (Fig. 5b) and with an inhibitor (Fig. 5c).

From Fig. 6, we can see that the percentage of iron in the steel sample in the

sintered solution was 87.3%. This indicates that the inhibitor showed a high level of protection of steel.

Fig. 7 shows the SEM photograph taken in the inhibitor-free solution, and we can see that the erosion on the outer surface has progressed to a high degree. It is also known from the elemental analysis presented in Fig. 7 that the corrosion has gone to a high level, where the percentage of iron is 59.8% [24, 25].



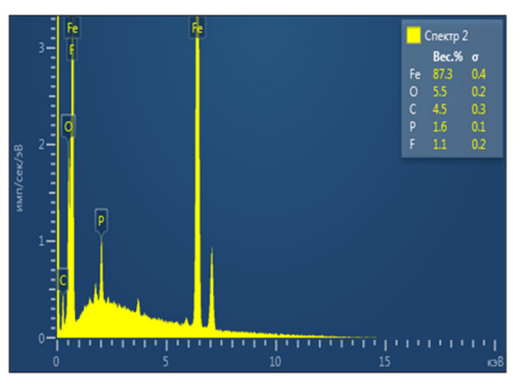
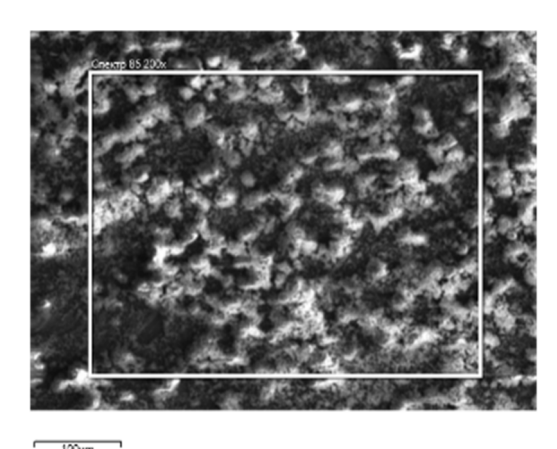


Fig 6. SEM and elemental analysis of St20 sample inhibited with PFG brand inhibitor



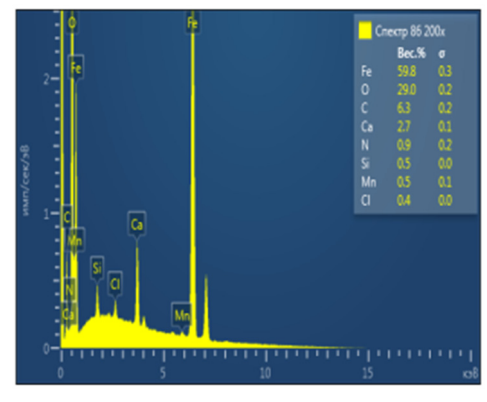
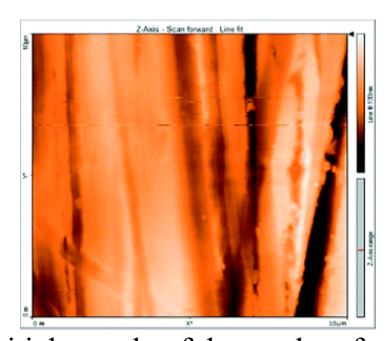


Fig 7. SEM photograph of an unannealed steel sample

AFM analysis. The morphology of the steel surface was further investigated using atomic force microscopy (AFM) (Fig. 8). Steel 20 samples, shaped as plates, were immersed in a 1M HCl solution for 24 hours, both with and without the PFG inhibitor. The surface

morphology was then analyzed using an Agilent 5500 atomic force microscope (Agilent, USA). The results showed that the clean steel sample had an almost flat surface, with no signs of corrosion.



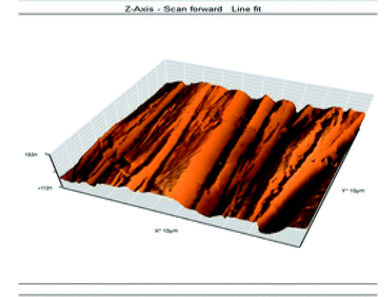


Fig 8. Initial sample of the steel surface obtained by atomic force microscopy

From Fig. 9, we can see that there is corrosion on the steel surface. Fig. 10 shows the state of the steel surface in the presence of the composite inhibitor PFG in a 1 M HCl solution for 24 hours. It can be seen that the steel surface is flat and has not undergone any corrosion

changes. Thus, the surface morphology of steel 20 samples immersed in 1M HCl solution for 24 hours and immersed in 1 M HCl solution for 24 hours in the presence of inhibitor PFG was studied and analyzed in (3D) form using atomic force microscopy method [26-29].

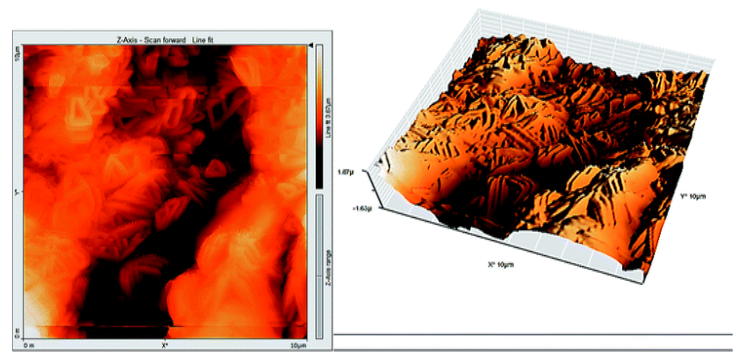
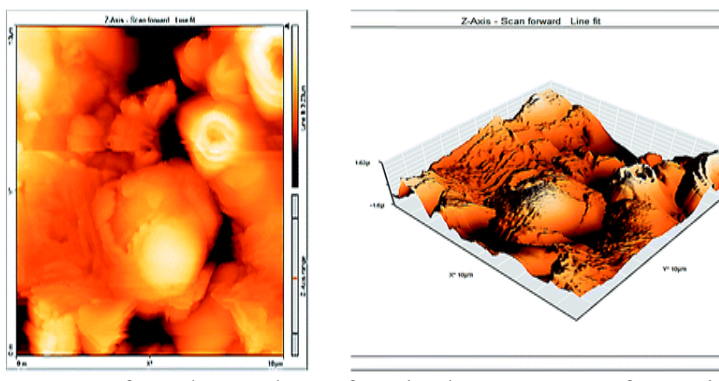


Fig 9. Sample of the without inhibitor in a 1M HCl environment



**Fig 10.** The appearance of steel sample surface in the presence of PFG inhibitor in 1M HCl solution.

#### Conclusion

Optimal conditions for synthesizing a PFG-brand corrosion inhibitor, derived from p-phenylenediamine, formalin, and glycine, were investigated. Analysis of the synthesized inhibitor using IR spectroscopy revealed characteristic peaks at 3480.52 cm<sup>-1</sup>, 3366.81 cm<sup>-1</sup>, and 3217.83 cm<sup>-1</sup>, corresponding to the symmetric v(NH) valence and  $\delta$  deformation vibrations, while peaks at 1505.29 cm<sup>-1</sup> and 1469.20 cm<sup>-1</sup> indicated the presence of additional functional groups. The absorption band at 1630.09 cm<sup>-1</sup> was attributed to the v(C=O) stretching vibration, and peaks around 836.57 cm<sup>-1</sup> corresponded to both valence and

deformation vibrations.

Quantum chemical analyses, including HOMO-LUMO calculations, were performed to further study the electronic properties and reactivity of the inhibitor molecule. Gravimetric measurements in a 1 M HCl solution at concentrations of 200, 400, 600, and 1000 mg/L showed an inhibition efficiency of 93.82%. Additionally, the inhibitor's impact on the steel surface was evaluated using SEM and AFM imaging techniques. Overall, the findings demonstrate that the PFA-brand corrosion inhibitor is highly effective in a 1 M HCl environment.

#### Acknowledgment

Authors thanks to *Termez State University of Engineering and Agrotechnology* and Termez branch of Tashkent Medical Academy the for support this research work.

## Disclosure statement

The authors declare no conflict of interest.

- Conflicts of Interest: None.
- I/We hereby confirm that all the Figures and Tables in the manuscript are mine/ours. Furthermore, any Figures and images, that are not mine/ours, have been included with the necessary permission for re-publication, which is attached to the manuscript.

- No animal studies are present in the manuscript (Only if the author did not use laboratory animal in his/her research).
- No human studies are present in the manuscript (Authors who did not present manuscripts reporting studies involving human participants, human data or human tissue).
- Ethical Clearance: The project was approved by the local ethical committee at Termez State University of Engineering and Agrotechnology

# **Source of Funding**

This article is funded by Termez State University of Engineering and Agrotechnologies.

## References

- Lagrenée M., Mernari B., Bouanis M., Traisnel M., Bentiss F. Study of the mechanism and inhibiting efficiency of 3,5-bis(4-methylthiophenyl)-4H-1,2,4-triazole on mild steel corrosion in acidic media. *Corros. Sci.*, 2002, Vol. 44(3), p. 573–588. <a href="https://doi.org/10.1016/S0010-938X(01)00075-0">https://doi.org/10.1016/S0010-938X(01)00075-0</a>.
- Ostanov U.Y., Beknazarov Kh.S., Dzhalilov A.T. Study By Differential Thermal Analysis and Thermogravimetric Analysis of the Heat Stability of Polyethylene Stabilised With Gossypol Derivatives. *Inter Polymer Sci. and Tech.* 2011, Vol. 38(9), p. 25–27. <a href="https://doi.org/10.1177/0307174X110380090">https://doi.org/10.1177/0307174X110380090</a>
   6.
- 3. Nurilloev Z., Beknazarov Kh., Nomozov A. Production of Corrosion Inhibitors Based on Crotonaldehyde and Their Inhibitory Properties. *Int. J. of Eng. Trends and Tech.* 2022, **Vol. 70(8)**, p. 423-434. <a href="https://doi.org/10.14445/22315381/IJETT-V7018P243">https://doi.org/10.14445/22315381/IJETT-V7018P243</a>.
- 4. Narzullaev A.X., Beknazarov X.S., Jalilov A.T., Rajabova M.F. Studying the Efficiency of Corrosion Inhibitor IKTSF-1, IR-DEA, IR-DAR-20 in 1m HCl. *Inter. J. of Advan. Sci. and Tech.* 2019, **Vol. 28(15)**, p. 113–122.
  - http://sersc.org/journals/index.php/IJAST/article/view/1555.
- 5. El-Sonbati A.Z., Diab M.A., Abou-Dobara M.I., Eldesoky A.M., Issa H.R. Synthesis, characterization, electrochemical studies and antimicrobial activities of metal complexes. *J. Iran. Chem. Soc*, 2021, **Vol. 19(3)**, p. 979–1002. <a href="https://doi.org/10.1007/s13738-021-02354-1">https://doi.org/10.1007/s13738-021-02354-1</a>
- 6. Beknazarov K.S., Dzhalilov A.T. The

- Synthesis of Oligomeric Derivatives of Gossypol and the Study of their Antioxidative Properties. *Inter. Poly. Sci. and Tech.* 2016, **Vol. 43(3)**, p. 25–30. https://doi.org/10.1177/0307174X160430030
- 7. Du T., Chen J., Cao D. N,N-Dipropynoxy methyl amine trimethyl phosphonate as corrosion inhibitor for iron in sulfuric acid. *J. Mater. Sci.* 2001, Vol. 36(16), p. 3903–3907. <a href="https://doi.org/10.1023/A:1017909919388">https://doi.org/10.1023/A:1017909919388</a>
- 8. Ugryumov O.V., Ivshin Ya.V., Fakhretdinov P.S., Romanov G.V., Kaidrikov R.A. N-[Isononylphenoxypoly(ethyleneoxy)carbonyl methyl]ammonium Chlorides as Inhibitors of Metal Corrosion. I. Inhibition of Steel Corrosion in Aqueous Hydrochloric Media. *Prot. Met.* 2001, **Vol.** 37(4), p. 337–342. https://doi.org/10.1023/A:1010491325583
- 9. Palomar M.E., Olivares-Xometl. C.O., Likhanova N.V., Pérez-Navarrete J.-B. Imidazolium, Pyridinium and Dimethyl-Ethylbenzyl Ammonium Compounds as Mixed Corrosion Inhibitors in Acidic Medium. J. Surfactants Deterg. 2010, 211-220. Vol. 14(2), p. https://doi.org/10.1007/s11743-010-1236-1
- 10. Abdel Hameed R.S., Abdallah M. Corrosion Inhibition of Carbon Steel in 1 M Hydrochloric Acid using Some Pyrazolo[3,4-d]Pyrimidnone Derivatives. *Physicochemical Problems of Materials Protection*, 2018, **Vol. 54(1)**, p. 113–121. <a href="https://doi.org/10.1134/S207020511801023">https://doi.org/10.1134/S207020511801023</a>
- 11. Beknazarov Kh.S., Dzhalilov A.T. Protection of steel from corrosion by oligomeric inhibitors and their compositions. *Chem and Chem Tech.* 2015, **Vol. 1**, p. 50-52.

- 12. Selvi J.A., Arthanareeswari A., Pushpamalini T., Rajendran S., Vignesh T. Effectiveness of Vinca rosea leaf extract as corrosion inhibitor for mild steel in 1 N HCl medium investigated by adsorption and electrochemical studies. *Int. J. Corros. Scale Inhb.*, 2020, **Vol. 9(4)**, p. 1429–1443. <a href="https://doi.org/10.17675/2305-6894-2020-9-4-15">https://doi.org/10.17675/2305-6894-2020-9-4-15</a>.
- 13. Fouda A.S., Abd El-Maksoud A.S., Zoromba M.Sh., Ibrahim A.R. Corrosion Inhibition and thermodynamic activation parameters of Myrtus communis extract on mild steel in sulfamic and medium. *Int. J. Corros. Scale Inhib.* 2017, **Vol. 6(4)**, p. 428–448. <a href="https://doi.org/10.17675/2305-6894-2017-6-4-4">https://doi.org/10.17675/2305-6894-2017-6-4-4</a>
- 14. Ghames A., Douadi T., Issaadi S., Sibous L., Alaoui K.I., Taleb M., Chafaa S. Theoretical and Experimental Studies of Characteristics of Newly Adsorption Synthesized Schiff Bases and their Evaluation as Corrosion Inhibitors for Mild Steel in 1 M HCl. Int. J. Electrochem. Sci., 2017, Vol. **12**. 4867-4897. p. https://doi.org/10.20964/2017.06.92.
- 15. Yadav D.K., Quraishi M.A. Application of Some Condensed Uracils as Corrosion Inhibitors for Mild Steel: Gravimetric, Electrochemical, Surface Morphological, UV–Visible, and Theoretical Investigations. *Ind. Eng. Chem. Res.*, 2012, **Vol. 51(46)**, p. 14966–14979.
  - https://doi.org/10.1021/ie301840y.
- 16. Muratov B.A., Turaev Kh.Kh., Umbarov I.A., Kasimov Sh.A., Nomozov A.K. Studying of Complexes of Zn(II) and Co(II) with Acyclovir (2-amino-9-((2-hydroxyethoxy)methyl)-1,9- dihydro-6H-purine-6-OH). *Int. J of Eng. Trends and Tech.* 2024, **Vol. 72(1)**, p. 202-208. <a href="https://doi.org/10.14445/22315381/IJETT-V72IIP120">https://doi.org/10.14445/22315381/IJETT-V72IIP120</a>.
- 17. Nomozov A.K., Beknazarov Kh.S., Khodjamkulov S.Z., Misirov Z.K. Salsola Oppositifolia acid extract as a green corrosion inhibitor for carbon steel. *Indian J Chem Tech.* 2023, Vol. 30(6), p. 872-877. https://doi.org/10.56042/ijct.v30i6.6553
- 18. Majed R.A. Corrosion Inhibition of Al-Si-Cu Alloy in the Basic Media by Using Six

- Inhibitors at Four Temperatures. *Baghdad Sci. J.* 2008, **Vol. 5(3)**, p. 427-36. <a href="https://bsj.uobaghdad.edu.iq/index.php/BSJ/article/view/921">https://bsj.uobaghdad.edu.iq/index.php/BSJ/article/view/921</a>.
- Qiang Y., Zhang S., Xiang Q., Tan B., Li W., Chen S., Guo L. Halogeno-substituted indazoles against copper corrosion in industrial pickling process: a combined electrochemical, morphological and theoretical approach. *RSC Adv.* 2018, Vol. 8, p. 38860–38871. <a href="https://doi.org/10.1039/C8RA08238C">https://doi.org/10.1039/C8RA08238C</a>
- 20. Nomozov A.K. Spectrophotometric determination of copper(II) ion with 7-bromo-2-nitroso-1-oxinaphthalene-3,6-disulphocid. *Indian J of Chem.* 2024, **Vol.** 63(5), p. 500-505. <a href="https://doi.org/10.56042/ijc.v63i5.9289">https://doi.org/10.56042/ijc.v63i5.9289</a>.
- 21. Shaymardanova M., Mirzakulov Kh., Melikulova G., Khodjamkulov S., Nomozov A., Toshmamatov O. Studying of The Process of Obtaining Monocalcium Phosphate based on Extraction Phosphoric Acid from of Phosphorites Central Kvzvlkum. Baghdad Sci. J. 2024, Vol. 22(1), https://doi.org/10.21123/bsj.2024.9836.
- 22. Shaymardanova M.A., Mirzakulov Kh.Ch, Melikulova G., Khodjamkulov S.Z, Nomozov Shaymardanova Kh.S. Study of obtaining monopotassium processe phosphate based monosodium on phosphate and potassium chloride. Chemical Problems. 2023, Vol. 21(3), https://doi.org/10.32737/2221-8688-2023-3-279-293.
- 23. Yulchieva M.G., Turaev Kh.Kh., Nomozov A.K., Tovoshareva I.E. Studying synthesis of a chelate-forming sorbent based on ureaformaldehyde and diphenylcarbazone. *Indian J of Chem*, 2024, **Vol. 63**, p. 579-585.
  - https://doi.org/10.56042/ijc.v63i6.9006.
- 24. Turaev Kh.Kh., Eshankulov Kh.N., Umbarov I.A., Kasimov Sh.A., Nomozov A.K., Nabiev D.A. Studying of Properties of Bitumen Modified based on Secondary Polymer Wastes Containing Zinc. *Inter J. of Engin. Trends and Tech.* 2023, **Vol. 71(9)**, p. 248-255. <a href="https://doi.org/10.14445/22315381/IJETT-V71I9P222.">https://doi.org/10.14445/22315381/IJETT-V71I9P222.</a>

- 25. Al-Naemi A.N., Abdul-Majeed M.A., Al-Furaiji M.H., Ghazi I.N. Fabrication and Characterization of Nanofibers Membranes Using Electrospinning Technology for Oil Removal. *Baghdad Sci J.* 2021, **Vol. 1(4)**, p. 1338-1343. https://doi.org/10.21123/bsj.2021.18.4.1338
- 26. Nomozov A.K., Eshkaraev S.Ch., Jumaeva Z.E., Todiiev J.N., Eshkoraev Umirqulova F.A. Experimental Theoretical Studies of Salsola oppositifolia Extract as a Novel Eco-Friendly Corrosion Inhibitor for Carbon Steel in 3% NaCl. Inter J of Engin Trends and Tech. 2024, Vol. 72(9), 312-320. p. https://doi.org/10.14445/22315381/IJETTV 72I9P126.
- 27. Muzaffarova N.Sh., Nurkulov F.N., Khaydarova Z.N., Abdirazokov A., Bozorova M.I., Abdimalikov I.I. Synthesis of fire retardant with phosphorus and metal

- for preservation and reach of reduction of flammability of textile materials. *Chemical Problems*. **Vol. 22(3)**, 2024, p. 290-302. <a href="https://doi.org/10.32737/2221-8688-2024-3-290-302">https://doi.org/10.32737/2221-8688-2024-3-290-302</a>.
- 28. Mammadli S.B., Amirov F.A., Alamdarly A.V., Orucaliyeva U.B., Nurullayeva D.R. Synthesis of an optically transparent copolymer on the basis of n-vinyl carbazole and styrene. *Chemical Problems*. 2022, Vol. 20(4), p.374-380. <a href="https://doi.org/10.32737/2221-8688-2022-3-374-380">https://doi.org/10.32737/2221-8688-2022-3-374-380</a>.
- 29. Muqimov A., Turaev Kh.Kh., Tojiev P.J., Nabiev D.A., Nomozov A. Modern approach to the addition of organomineral additives to increase cement brand. A review. *Chemical Review and Letters*. 2024, Vol.7(9) p.804-815. <a href="https://doi.org/10.22034/crl.2024.467805.1">https://doi.org/10.22034/crl.2024.467805.1</a> 381